

Detection of heavy Majorana neutrinos and right-handed bosons

S. N. Gninenko^{i*}; M. M. Kirsanov^{i†}; N. V. Krasnikov^{i‡}; V. A. Matveevⁱ

ⁱ *INR Moscow*

June 5, 2007

Abstract

The $SU_C(3) \otimes SU_L(2) \otimes SU_R(2) \otimes U(1)$ left-right (LR) symmetric model explains the origin of the parity violation in weak interactions and predicts the existence of additional gauge bosons W_R and Z' . In addition, heavy right-handed Majorana neutrino states N arise naturally within LR symmetric model. The N s could be partners of light neutrino states, related to their non-zero masses through the see-saw mechanism. This makes the searches of W_R , Z' and N interesting and important.

In the framework of the minimal LR model we study the possibility to observe signals from N and W_R production in pp collisions after three years of running at low LHC luminosity. We show that their decay signals can be identified with a small background, especially in the case of same-sign leptons in the final state. For the integral LHC luminosity of $L_t = 30 \text{ fb}^{-1}$, the 5σ discovery of W_R - boson and heavy Majorana neutrinos N_e with masses M_{W_R} up to 4 TeV and M_{N_e} up to 2.4 TeV respectively is found possible.

1 Introduction

Among several extensions of the Standard Model (SM) that can be tested at LHC, see e.g. [1], the left-right (LR) symmetric model $SU_C(3) \otimes SU_L(2) \otimes SU_R(2) \otimes U(1)$ [2] is certainly one of the most interesting. The model embeds the SM at the scale of the order of 1 TeV and naturally explains the parity violation in weak interactions as a result of the spontaneously broken parity. The model necessarily incorporates three additional gauge bosons W_R and Z' and the heavy right-handed Majorana neutrino states N . The N s can be the partners (N_l) of the light neutrino states ν_l ($l = e, \mu, \tau$) and can provide their non-zero masses through the see-saw mechanism [3]. This makes LR model very attractive, since recent results from atmospheric, solar and reactor neutrino experiments confirm the existence of neutrino oscillations, see e.g. [4], and therefore provide strong evidence that neutrinos are not massless. The above mentioned experiments, though very impressive, provide no hints neither on the nature of the masses (i.e. they cannot distinguish Dirac and Majorana neutrinos) nor on their values. The only observation that can be used to give preference to some models as compared to others is the fact that the neutrino masses are very small as compared to the charged lepton and quark masses. On the contrary, experiments searching for signals from N s with masses in the LHC energy range look quite promising, since the large number of extensions of the LR model predict the heavy neutrino masses to be somewhere between several hundred GeV and a few TeV [1].

There are several recent papers devoted to the study of the production of heavy neutrinos and new gauge bosons at TeV energy scale, see e.g. Ref. [5]- [9]. In this paper we discuss

* **e-mail:** Sergei.Gninenko@cern.ch

† **e-mail:** Mikhail.Kirsanov@cern.ch

‡ **e-mail:** Nikolai.Krasnikov@cern.ch

the production and the experimental signature of heavy Majorana neutrinos and the associated heavy gauge bosons in the CMS detector at LHC. We perform our study in the framework of the minimal LR symmetric model [2].

Among several reactions of N and W_R production in pp collisions the most interesting are: i) $p + p \rightarrow 2l^\pm + X$ due to the W_R fusion mechanism, ii) $p + p \rightarrow W_R + X \rightarrow N_l + l + X$ and iii) $p + p \rightarrow 2N_l + X$ with the subsequent decay of N_l 's into charged leptons l and jets. The first reaction is quite similar to the process of lepton number violation in the double- β decay and has a clear experimental signature as an advantage. However, its cross-section is small as compared to the processes ii) and iii) [5]. The goal of the work is to examine how the direct production of W_R and N in reactions ii) at the LHC energy can be manifested through charged lepton pairs accompanied by high P_t jets. The Majorana nature of heavy neutrino N reserves possibilities of an excellent cross check or a dramatic suppression of the background since in 50% of events the signal leptons will have the same sign. We also discuss the optimal conditions for the observation of W_R and N signals in CMS at low luminosity taking into account all relevant background sources.

The rest of the paper is organized as follows. In Section 2 we briefly remind the essence of the LR model and some constraints on its parameters. The description of the CMS detector components relevant for the present study is presented in Section 3. In Sections 4 - 7 we consider the production and decays of W_R and N_l at LHC and backgrounds for their detection, respectively. In Section 8 we estimate the CMS discovery potential for the process $pp \rightarrow W_R \rightarrow eN_e$. Section 9 contains concluding remarks.

2 Left-right symmetric models

LR symmetric models of electroweak interactions were proposed to explain the origin of parity nonconservation in weak interactions [2]. It is well known that in the SM gauge symmetry is broken spontaneously, while parity (and charge) conjugation is broken explicitly in the Lagrangian. In the LR symmetric model parity, in contrary, is conserved in the Lagrangian and broken spontaneously together with the gauge symmetry.

An important question for the phenomenology of these models is the scale of the parity breaking. During a long time there has been an interest in models where the masses of the right handed W_R and Z' are in the multi-TeV region. With the recent discovery of non-zero neutrino masses, the case for left-right models has become more compelling for two reasons: i) the right handed neutrino, which is necessary to implement the see-saw mechanism, is an integral part of these models and ii) the local $B - L$ symmetry which protects the right handed neutrino mass from being at the Planck scale is also part of the gauge symmetry.

In the minimal $SU(2)_L \times SU(2)_R \times U(1)_{B-L}$ model each generation of quarks and leptons carry the quantum numbers $Q_L \sim (1/2, 0, 1/3)$, $Q_R \sim (0, 1/2, 1/3)$, $L_L \sim (1/2, 0, -1)$, $L_R \sim (0, 1/2, -1)$. The right-handed fields are doublets under $SU(2)_R$ and a right-handed neutrino N_R should exist. The minimal Higgs sector consists of a bi-doublet $\phi \sim (1/2, 1/2, 0)$ and two triplets $\Delta_R \sim (1, 0, 2)$, $\Delta_L \sim (0, 1, 2)$. After the spontaneous symmetry breaking, the phenomenological requirement $|v_L| \gg |k_1|, |k_2| \ll |v_R|$ for the vacuum expectation values $v_{L,R}$ and $k_{1,2}$ of the triplet and doublets Higgs fields ensures the suppression of the right-handed currents and the smallness of the neutrino mass.

The $SU(2)_L \times SU(2)_R \times U(1)_{B-L}$ gauge symmetry group implies that the usual left-handed gauge bosons $W_L^i (i = 1, 2, 3)$, their right-handed counterparts W_R^i and the $U(1)$ gauge boson Y combine to form the physical charged and neutral gauge bosons and the photon. In general, the strength of the gauge interactions of these bosons is described by the coupling constants g_L , g_R and g' , respectively. However, strict LR symmetry $\Phi_L \leftrightarrow \Phi_R$, $\Delta_L \leftrightarrow \Delta_R$, $\phi \leftrightarrow \phi^+$, where Φ denotes fermions, leads to the relation $g_L = g_R$, which will be assumed throughout this paper.

The weak eigenstates W_L^\pm and W_R^\pm mix in the mass eigenstates W^\pm and W'^\pm . Assuming CP invariance, the mixing matrix is defined by the angle ξ_W :

$$\begin{aligned} W^\pm &= \cos\xi_W W_L^\pm + \sin\xi_W W_R^\pm \\ W'^\pm &= -\sin\xi_W W_L^\pm + \cos\xi_W W_R^\pm \end{aligned} \quad (1)$$

The weak eigenstate W_L can be identified with the pure SM gauge boson. Similarly the neutrino mass eigenstates are mixtures of the weak eigenstates, parametrized by the angle ξ_N :

$$\begin{aligned} \nu &= \cos\xi_N \nu' + \sin\xi_N N' \\ N &= -\sin\xi_N \nu' + \cos\xi_N N' \end{aligned} \quad (2)$$

Here, ν and N are the light and heavy neutrino mass eigenstates, and $\nu' = \nu_L + \nu_L^c$ and $N' = \nu_R + \nu_R^c$ are the usual self-conjugate spinors. For simplicity, we do not take into account possible mixing between generations.

The charge-current interactions vertexes for the left-chiral and right-chiral currents are given by

$$\begin{aligned} \langle \nu_L | W_L | e^- \rangle &= g/2\sqrt{(2)} W_L^{+\mu} \bar{\nu}_L \gamma_\mu (1 - \gamma_5) e \\ \langle N_R | W_R | e^- \rangle &= g/2\sqrt{(2)} W_R^{+\mu} \bar{N}_R \gamma_\mu (1 + \gamma_5) e \end{aligned} \quad (3)$$

The charge-current interactions for the mixed mass eigenstates can be obtained from these matrix elements.

The neutral gauge bosons in L-R models are mixtures of $W_{L,R}^3$ and Y . The mixing between the massive neutral bosons can be parametrized as

$$\begin{aligned} Z &= \cos\xi_Z Z_1 + \sin\xi_Z Z_2 \\ Z' &= -\sin\xi_Z Z_1 + \cos\xi_Z Z_2 \end{aligned} \quad (4)$$

where Z and Z' denote the mass eigenstates, and Z_1 and Z_2 denote the weak eigenstates of the massive neutral bosons. The field Z can be identified as the corresponding SM boson.

The tree-level neutral current interaction for the physical Z, Z' is of the form

$$L_{NC} = g/2\cos\Theta_W [\bar{f}\gamma_\mu (g_V^f - g_V^f\gamma_5) f Z_\mu + \bar{f}\gamma_\mu (g_V^{\prime f} - g_V^{\prime f}\gamma_5) f Z'_\mu] \quad (5)$$

where

$$\begin{aligned} g_V^f &= \cos\xi_Z g_V^{0f} + \sin\xi_Z g_V^{\prime f}, \\ g_A^f &= \cos\xi_Z g_A^{0f} + \sin\xi_Z g_A^{\prime f} \end{aligned} \quad (6)$$

and

$$g_V^{0f} = I_3^f - 2Q^f \sin^2 \Theta_W, \quad g_V^{\prime f} = \sqrt{\cos 2\Theta_W} g_V^{0f}$$

$$g_A^{0f} = I_3^f, \quad g_A^{\prime f} = -\sqrt{\cos 2\Theta_W} g_A^{0f} \quad (7)$$

Here we take into account that in the LR model $I_{3R}^f = I_{3L}^f \equiv I_3^f$ for the third components of the L/R isospin for a given fermion flavor f .

Existing experimental data constrain the Z' mass to the values $O(1)$ TeV and the mixing among the neutral gauge bosons to the values below $O(10^{-4})$ [10, 11].

The lower bound on the W' mass derived from the $K_L - K_S$ mass difference is quite stringent, $M_{W'} \gtrsim 1.6$ TeV [12], however with some uncertainties from the low energy QCD corrections to the kaon system. The bound on the mixing angle is as low as $\xi_W \lesssim 0.013$ [13]. The direct searches for W' at the Tevatron yield bounds $M_{W'} \gtrsim 720$ GeV assuming a light (keV-range) N , and $M_{W'} \gtrsim 650$ GeV assuming $M_N < M_{W'}/2$ [14]. These bounds are less stringent in more general LR models [15].

The least tested components of the LR model are the masses and mixings of neutrinos. The analysis of the precision data constrains fermion mixings [16]: the 90% CL bound for the electron neutrinos is $|\xi_N| \lesssim 0.081$.

The mixing angle ξ_W is independent on the neutral current parameters. The value of ξ_N depends rather strongly on the parameters of the model, allowing mixings up to $\xi \simeq 0.1$ [17].

3 The CMS Detector

The CMS detector is designed to search for signals of new physics at LHC at a nominal luminosity up to $10^{34} \text{ cm}^{-2}\text{s}^{-1}$ [18]. The detector consists of a number of sub-detectors most of which are located inside a 4T superconducting solenoid with a volume of about 3 m in diameter and 5 m long. Their features relevant for the present study will be briefly mentioned. The inside surface of the internal volume is instrumented all around with ~ 61000 PWO crystal in the Barrel and ~ 15000 PWO crystals in Endcaps of the electromagnetic calorimeter [19]. The ECAL surrounds the inner silicon tracker and is followed by a scintillator-iron hadronic calorimeter [20] and a muon spectrometer [21].

The energy of an isolated electron (or photon) is expected to be measured in the ECAL with an accuracy [19]

$$\delta(E)/E \simeq ((5\%/\sqrt{E})^2 + (\delta_{noise})/E)^2 + (0.5\%)^2)^{1/2}, \quad \text{for } |\eta| < 2.5, \quad (8)$$

where $\delta_{noise} \simeq 0.2$ GeV is the noise coefficient, and E is in GeV.

The isolated electron identification efficiency is assumed to be close to 100%. The probability to misidentify the electron charge sign in the inner tracker varies from $\simeq 1\%$ at $p_T = 500$ GeV/c to $\simeq 15\%$ for $p_T = 2$ TeV/c.

A calorimeter object not identified as the electron(positron) or photon is considered as a hadron or jet with its energy measured in conjunction with the hadron calorimeter with an accuracy [20]

$$\delta(E)/E \simeq ((100\%/\sqrt{E})^2 + (5\%)^2)^{1/2} \quad \text{for } |\eta| < 3 \quad (9)$$

and

$$\delta(E)/E \simeq ((172\%/\sqrt{E})^2 + (9\%)^2)^{1/2} \quad \text{for } |\eta| > 3 \quad (10)$$

In the first year of running with reduced intensity the integral LHC luminosity is expected to be about 10 fb^{-1} .

The assembling of the detector was started in 2005 at the intersection point near Cessy. It is performed first on the ground level. The bigger parts of the detector will then be lowered underground. As of the end of 2005 the main parts like muon chambers, ECAL and HCAL support structures are well visible. The first test runs are expected in 2007.

4 Heavy Majorana neutrino production and decay

One can study at LHC two kinds of processes with W_R and N_l [5, 6]: $pp \rightarrow W_R \rightarrow l + N_l + X$, and $pp \rightarrow Z' \rightarrow N_l + N_l + X$ followed by the decay $N_l \rightarrow l + j_1 + j_2$. The corresponding Feynman diagrams are shown in Figure 1. The cross sections of these processes depend on the following parameters:

- the value of the coupling constant g_R ,
- parameters of the CKM mixing matrix for the right-handed sector,
- the $W_R - W_L$ and $Z' - Z$ mixing strengths, and
- the masses of the partners N_l of the light neutrino state.

To simplify our study, we will use the following standard assumptions:

- the mixing angles are small
- right-handed CKM matrix is identical to the left-handed one
- $g_R = g_L$

Under these conditions and given the Higgs sector with Majorana masses for neutrinos, Z' is about 1.7 times heavier than W_R . For this reason the process going through Z' has smaller cross section. In addition, its signature is more complicated. We limit our study to the process going through the W_R direct production.

Our additional assumption throughout this analysis is that only M_{N_e} is reachable at LHC, other N_l masses being very big. Hence we will have only electrons and positrons as leptons in the final states. The case with degenerated masses of N_l differs by the existence of reactions with muons and τ and by the additional factor in the cross section of the reaction $pp \rightarrow W_R \rightarrow e + N_e + X$ due to slightly different W_R branching ratio. This factor differs from unity by not more than 20%. Thus we will work with two parameters, namely M_{W_R} and M_{N_e} . **The point $M_{N_e} = 500$ GeV and $M_{W_R} = 2000$ GeV in this parameter space we will call below a reference point (LRRP).**

We used PYTHIA 6.2 [23] for the signal event generation and calculation of cross sections. PYTHIA 6.2 includes the LR symmetric model with the standard assumptions mentioned above. The default, CTEQ5L parton distribution functions of ref. [24] were used for calculations.

The dependence of the W_R total production cross section on its mass is shown in Figure 2. The fraction of $pp \rightarrow W_R^+$ ($pp \rightarrow W_R^-$) reactions as a function of M_{W_R} changes from $\simeq 70\%$ ($\simeq 30\%$) at $M_{W_R} \simeq 1$ TeV to $\simeq 95\%$ ($\simeq 5\%$) at $M_{W_R} \simeq 10$ TeV. Thus, at higher W_R boson masses the production of W_R^+ boson dominates.

As shown in Figure 1 the right-handed Majorana neutrino decays into a charged lepton l^\pm and an off-shell W_R boson which decays into a pair of quarks (jets (j) after hadronisation). This results in a final state $lljj$. In our case we have an electron from W_R (or positron, below will be called also electron) and the electron decay channel:

$$N_e \rightarrow eW_R^* \rightarrow e + 2 \text{ jets} \quad (11)$$

We study W_R mass region above 1 TeV, assuming that smaller masses are excluded by indirect analysis [6].

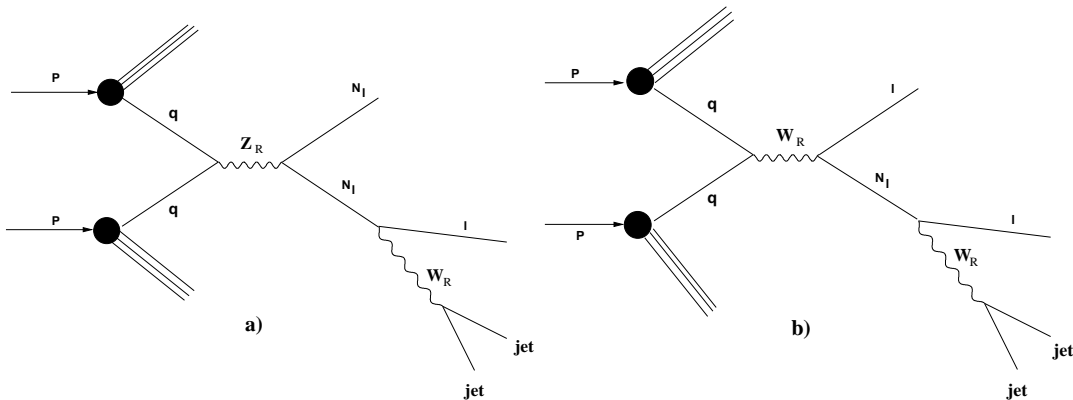


Figure 1: Feynman diagrams for production of the heavy neutrino through a) Z' bosons, b) W_R bosons.

The signal cross section, which is defined as the product of the total W_R production cross section and the branching ratio of W_R decay into electron and N_e , for different masses of W_R is shown in Figure 3 as a function of M_{N_e} . The production cross-section for $pp \rightarrow W_R \rightarrow eN_e$ was found to be at least one order of magnitude higher than for the $pp \rightarrow Z' \rightarrow N_e N_e$ process. Therefore, the channel $pp \rightarrow W_R \rightarrow eN_e$ is the best one for the heavy neutrino search.

5 The detector simulation and reconstruction

The detection of events with LR heavy neutrinos was studied using the full CMS detector simulation and reconstruction chain: CMKIN 4.3.1 (PYTHIA 6.227) \rightarrow OSCAR 3.6.5 \rightarrow ORCA 8.7.3. We use the following components of the latter: Trigger, ElectronPhoton code for the reconstruction of electrons, Jets and JetMET code for the reconstruction of Jets, Jets calibration and Missing E_t (MET) reconstruction.

We list below the main features and peculiarities of this analysis.

- Electrons (and positrons, below referred to also as electrons) are reconstructed by the ElectronPhoton code. We used both HLT and offline electrons (electrons that are reconstructed not necessarily at the place of a valid electron L1 trigger).
- We require that electrons should be isolated in tracker. This is very important: with the full simulation it becomes clear that it is not possible to use non-isolated electrons (as one could try do do in the simplified fast simulation, like widely used before CMSJET [22]) since they are found in most of jets. The isolation of electrons in the tracker was determined using the following criterion: not more than one charged particle with $P_t > 2$ GeV in the tracker in the cone with a radius of 0.3 around the electron track. The calorimeter isolation code based on towers was also created, but it turned out that, when applied after the tracker isolation selection, it practically does not improve the purity of electron sample. For this reason we applied it only with loose cuts.
- Jets are reconstructed by the JetsMet code (the Iterative Cone algorithm with GammaJet corrections and $R=0.5$). It gives satisfactory results at our LRRP.

6 Selection of candidate events and the analysis variables

In the analysis we proceeded through the following steps:

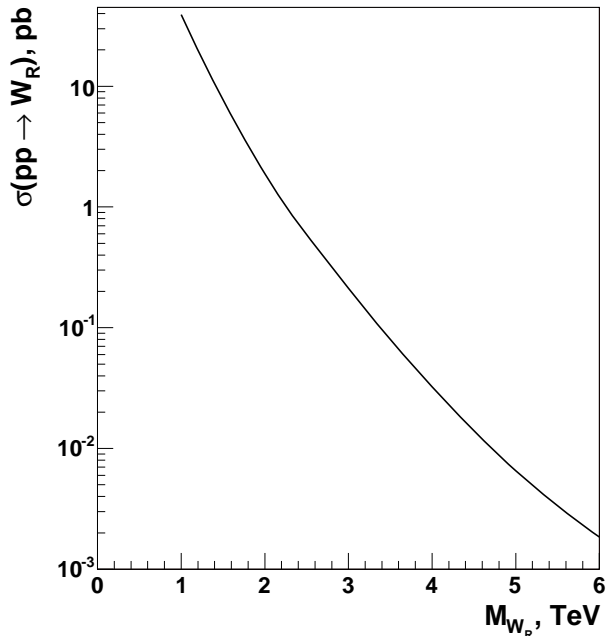


Figure 2: The dependence of the cross section $\sigma(pp \rightarrow W_R)$ on the W_R mass

- events with 2 isolated electrons are selected.
- events with at least 2 jets are selected. From these jets we select two jets with the maximal transverse momentum (signal jet pair). We found that for more than 90% of events we choose correct jets from the heavy neutrino decay if these jets are reconstructed (correct means that the jet is inside a cone of 0.05 radian around the quark of the PYTHIA event record produced in the decay of the heavy neutrino).
- using the 4-momenta of the signal jet pair and the 4-momentum of a lepton, the invariant mass $M_{ljj} = M_{N_e}^{cand}$ is calculated. Since we have two leptons, there are two ljj combinations and both of them should be considered. Finally, a peak in the distribution of this mass is to be searched for (Fig. 4).
- from the 4-momenta of the signal jet pair and the 4-momenta of electrons the invariant mass $M_{lljj} = M_{W_R}^{cand}$ is calculated. and a peak in the distribution of this mass is to be searched for, see Fig. 5.

Two more variables are used in the analysis:

- the minimal invariant mass of **all** same flavor lepton pairs M_{ll} . There is a lower cut on this value (typically $\simeq 200$ GeV)
- the E_t^{miss} of an event.

In Fig. 4 the $M_{N_e}^{cand}$ distribution is shown for the events simulated at LRRP. In Fig. 5 the distribution of $M_{W_R}^{cand}$ is shown for the same events.

The distributions are not symmetric. The additional broad peak or long tail above the heavy neutrino mass is due to the wrong choice of lepton. The long tail towards zero in the $M_{N_e}^{cand}$ distribution is due to the emission of gluons and to the heavy neutrino decay into t quark that produces wide jet or several jets.

In Figure 6 the efficiency of the primary selection and the efficiency of reconstruction of W_R decay products are shown. One can see that for neutrino masses much smaller than the W_R

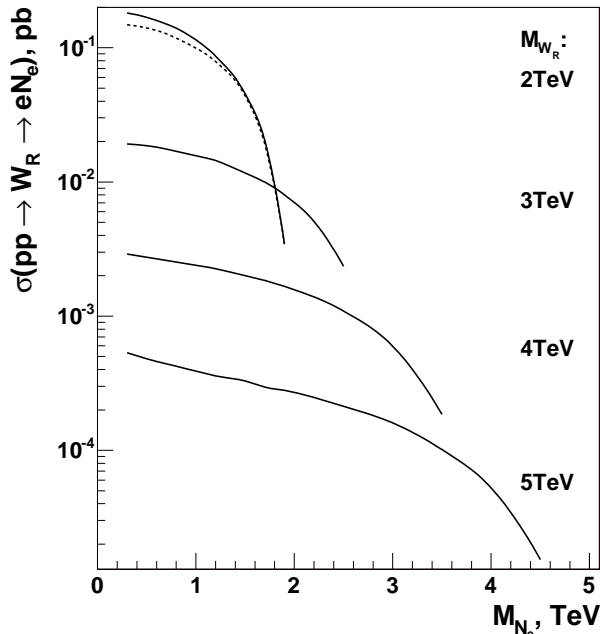


Figure 3: The dependence of the value $\sigma(pp \rightarrow W_R) \cdot Br(W_R \rightarrow e^\pm N_e)$ on the heavy neutrino mass. For $M_{W_R} = 2$ TeV the same value in case of degenerated N masses is shown by the dashed line.

mass the reconstruction efficiency drops. The reason is that the heavy neutrino decay products are too close to each other in the $\eta - \phi$ space. As a result, two jets are sometimes reconstructed as one, electron sometimes does not pass the isolation criteria. For very heavy W_R bosons (above 3 TeV) the drop of efficiency can even reduce the discovery region. Part of it can be recovered by changing in this mass region the selection criteria, namely by requiring one jet instead of two.

7 The background

The background is expected from the SM processes with a lepton pair and jets (two leading jets (from the diagram) or one leading jet and others from QCD effects). In the first approximation most of them can be simulated with PYTHIA.

To evaluate the amount of background, the events were processed by the same reconstruction program and passed the same selection criteria as signal events.

We considered the following sources of background.

The ZW production is the obvious source of background events. They were simulated with standard PYTHIA with lepton decay modes of W and hadron decay modes of Z forbidden. The cross section is of the order of the signal cross section at LRRP. The variable M_{ll} was used to suppress this kind of background. In ref [26] events with M_{ll} close to the Z mass central value were rejected. However, the tail of the Z mass distribution is rather long while signal events usually have a large value of M_{ll} . For this reason there was simply a lower cut on M_{ll} well above the Z mass central value (Fig. 7).

The $t\bar{t}$ production turned out to be one of the most important backgrounds. The simulation was made with PYTHIA and TOPREX [25]. This program correctly takes into account the spin correlations between the t and \bar{t} and uses TAUOLA code for τ decays. TOPREX gives $\approx 15\%$ smaller number of initial (with loose cuts) candidate events than PYTHIA. Only leptonic W decay modes were allowed (including $\tau\nu_\tau$). It was checked that other decay modes do not

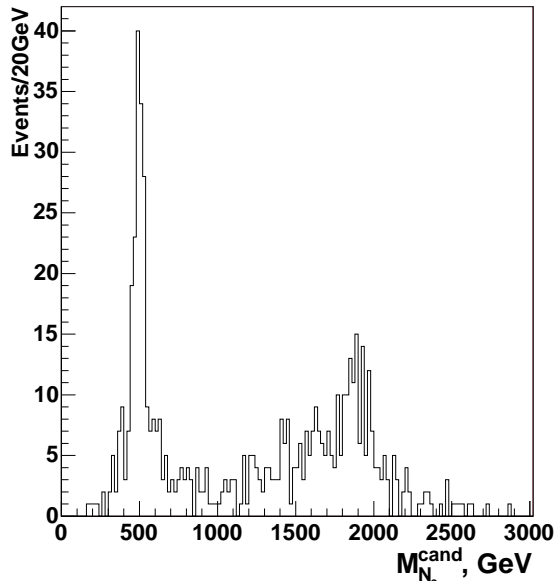


Figure 4: The distribution of the invariant mass $M_{N_e}^{cand}$ for the reconstructed events with a heavy neutrino. All combinations are shown. LRRP: the simulated neutrino mass is 500 GeV. The normalization is arbitrary

contribute. The cross section is about two orders of magnitude larger than the signal cross section at LRRP. For the cross section we used a PYTHIA value with a K factor of 1.2 and an additional factor of 1.24 to take into account diagrams with more particles in the final state, total factor 1.5. Preliminary studies with fast simulation showed that upper E_t^{miss} cut of the order of 25 - 30 GeV could be used to suppress this background. However, the first attempts to achieve such suppression with the full simulation and ORCA failed. In addition, our experience shows that E_t^{miss} is one of the most difficult physical values in the sense of reaching agreement between real data and MC. For this reason we decided not to use this cut.

Another important background is the $Z+jet$ process. This reaction has a large cross section: about 5 orders of magnitude larger than the signal cross section at LRRP. Even the simulation of events with event generator (PYTHIA was used), if simulated directly, would require a lot of CPU time. In order to reduce CPU time only events with $Q_t > 20$ GeV (PYTHIA parameter) were simulated. It was checked with loose cuts that the Q_t limit does not change the estimated number of background events for a given luminosity. This background is suppressed by the same cut as the ZW production and by the P_t cuts on leptons and jets. In Fig. 7 one can see the long tail of the Z invariant mass in this background process and how M_{ll} can be used for its suppression. It is also difficult to make directly a full simulation with sufficient statistics. For this reason only preselected events (less than 10^{-3} of all event generator events) were fully simulated.

The other possible sources of background are the ZH and WH productions. In our calculations we took $m_H = 190$ GeV. However, the cross sections are small and this background is not dangerous.

In Fig. 8 the reconstructed N_e mass peak in presence of the SM background is shown. The peak is well visible, though the background seems to be rather high in the mass region of several hundred GeV. However, if we require that in the same event there is a possibility to construct a heavy W_R boson candidate ($eejj$ system) with the invariant mass above 1 TeV, the background under the N_e peak drops dramatically, as can be seen from Fig. 9.

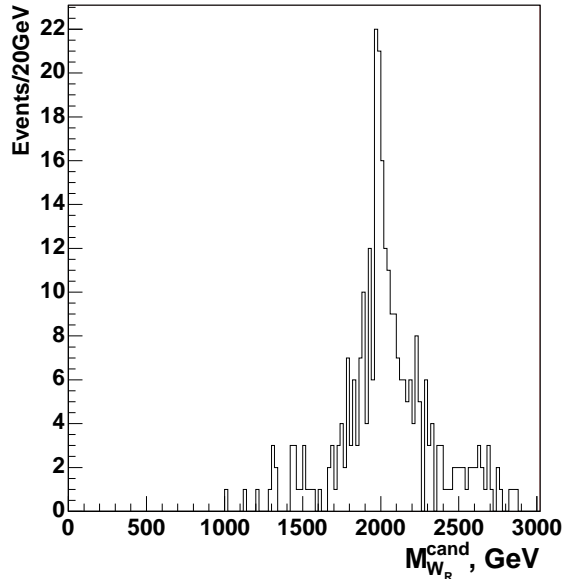


Figure 5: The distribution of the invariant mass $M_{W_R}^{cand}$ for the reconstructed events with a heavy neutrino. LRRP: the simulated W_R mass is 2000 GeV. The normalization is arbitrary

In Fig. 10 the reconstructed W_R mass peak in presence of the SM background is shown.

Table 1: Background reduction table. Primary selection requires two or more isolated leptons and two or more jets, checking leptons requires exactly two isolated leptons.

Step	Signal LRRP	$t\bar{t}$	Z + jet	ZW	WH
Initial	4965	2.2×10^6	6.2×10^7	6×10^4	11000
Primary selection	3505	1.2×10^5	-	38	728
Check leptons	2939	115000	-	15	165
M_{ll} cut	2830	13100	3870	0	72
Mass window	1211	2607	1000	0	2
Mass window + $M_{W_R} > 1$ TeV	1181	150	96	0	0

The Majorana nature of the heavy neutrino allows us to switch our analysis to same sign leptons. At the present stage of the analysis we see that in the parameter space to be studied (at least $M_{W_R} > 1$ TeV, lower values safely excluded by other experiments) this change does not improve the sensitivity because half of signal events are lost. However, in case of discovery this will be an excellent cross check.

The only found sources of events with same sign leptons that could be a background to the production of heavy Majorana neutrino are the ZH and WH productions. However, the cross section of these processes is small. For this reason the search for heavy neutrino events with the same sign leptons theoretically can be almost background-free.

More important background to the same sign analysis is the incorrect reconstruction of charge of electron tracks. We found that such tracks can be effectively suppressed by the lower cut on the number of hits in track. The cut at 6 hits was most appropriate, it gives a suppression

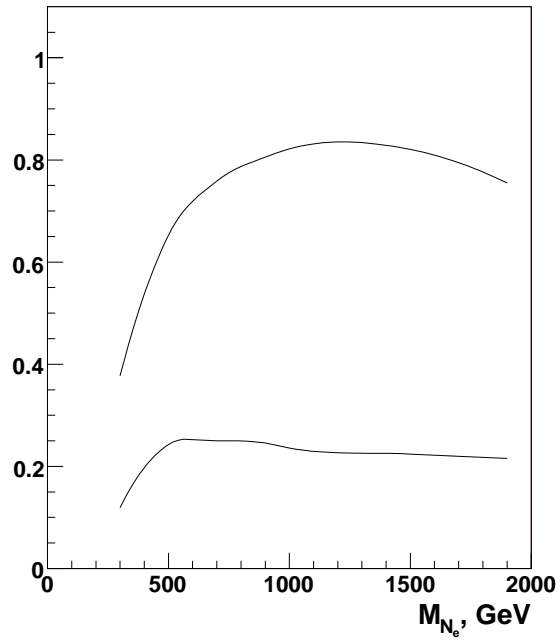


Figure 6: The probability to pass the primary selection for the $pp \rightarrow W_R \rightarrow e + N_e \rightarrow 2e + 2jet$ events as a function of the N_e mass for $M_{W_R} = 2$ TeV. The lower curve is the probability to have all four W_R decay products reconstructed as separate CMS reconstruction objects.

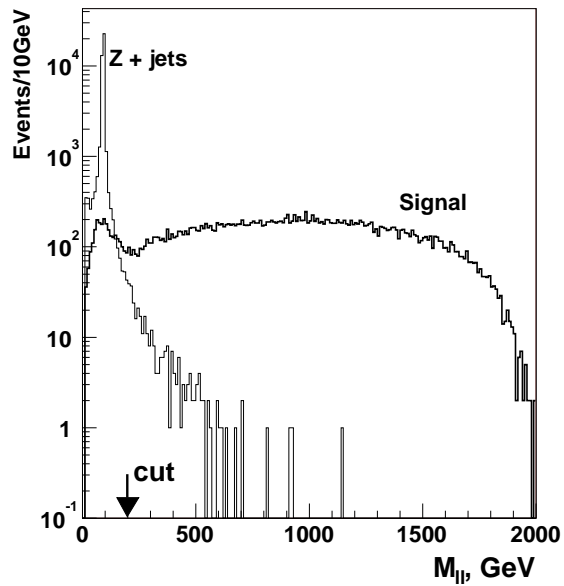


Figure 7: The use of the M_{ll} cut for the suppression of the Zg background

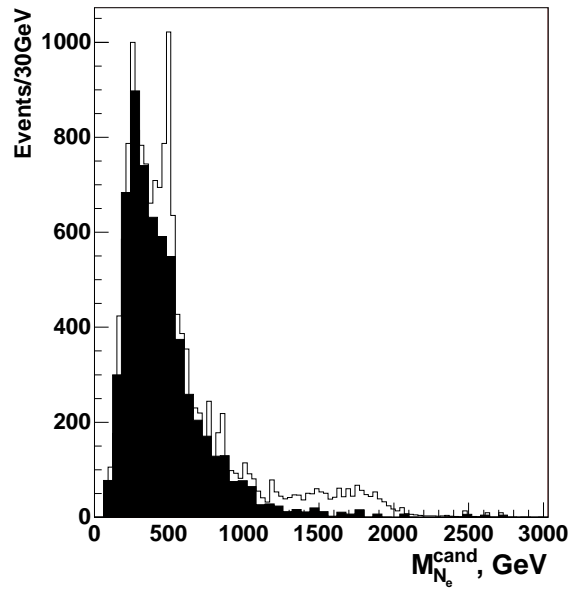


Figure 8: The heavy neutrino mass peak reconstructed together with the SM background (shaded histogram). $L_t = 30 \text{ fb}^{-1}$.

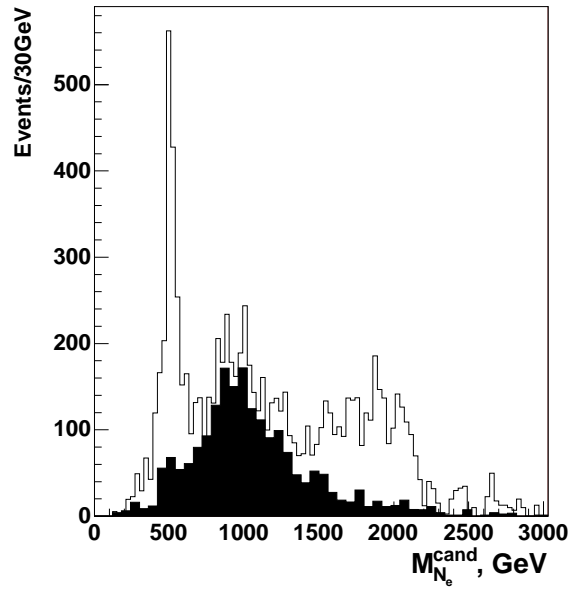


Figure 9: The heavy neutrino mass peak reconstructed together with the SM background (shaded histogram). The possibility to construct W_R with invariant mass above 1 TeV in the event is required. $L_t = 30 \text{ fb}^{-1}$.

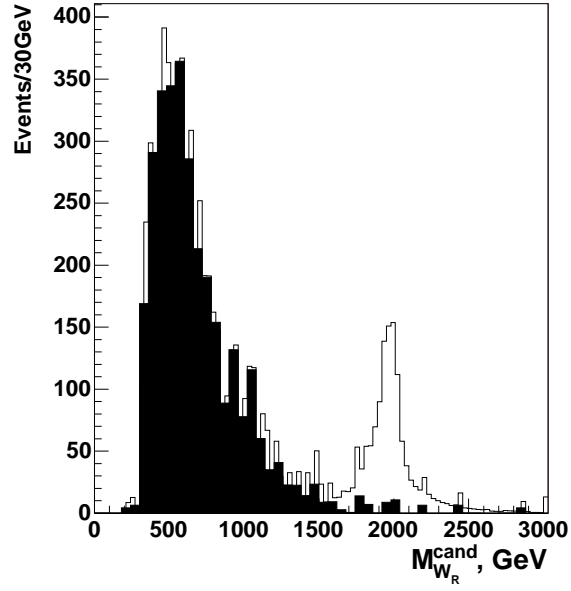


Figure 10: The W_R mass peak reconstructed together with the SM background (shaded histogram). $L_t = 30 \text{ fb}^{-1}$.

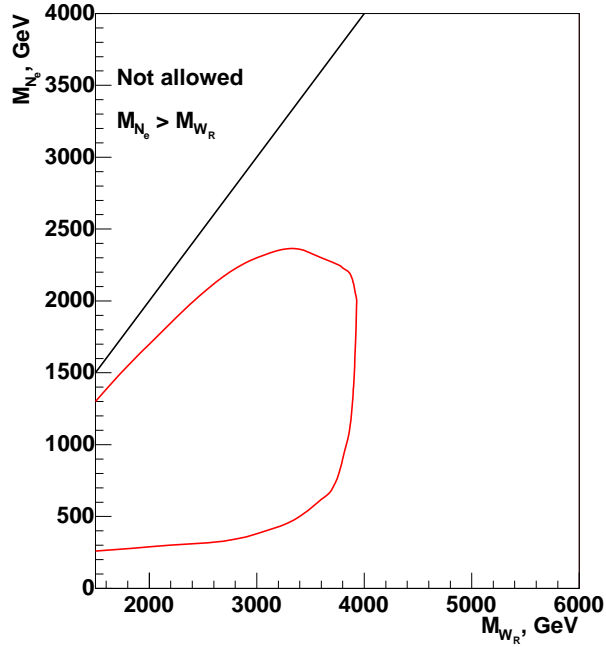


Figure 11: CMS discovery potential of the W_R boson and right-handed Majorana neutrinos of the Left-Right Symmetric model for the integrated luminosity $L_t = 30 \text{ fb}^{-1}$

factor of about 3 keeping the efficiency to tracks with a correct reconstruction on the level of 90%.

8 Results

The discovery potential of the events with W_R and N_e in CMS was calculated using the following relation [27]:

$$S = 2(\sqrt{N_S + N_B} - \sqrt{N_B}) \geq 5, \quad (12)$$

where N_S and N_B are the numbers of signal and background events respectively.

The corresponding discovery contour in the $(M_{W_R}; M_{N_e})$ plane is shown in Figure 11. After three years of running at low luminosity (30 fb^{-1}) the use of $pp \rightarrow W_R \rightarrow eN_e \rightarrow eejj$ reaction allows to discover W_R and N_e with masses up to 4 TeV and 2.4 TeV, respectively. For the LRRP point the corresponding significance is about 40.

9 Conclusion

We have studied the CMS potential to discover a heavy right-handed Majorana neutrino N_e and a heavy W_R gauge boson. For the integral luminosity of 30 fb^{-1} these new particles can be observed if M_{W_R} and M_{N_e} masses are less than 4 and 2.4 TeV respectively. At the LRRP point (masses 2 TeV and 500 GeV) W_R and N_e can be discovered already after one month of running at low luminosity.

The sensitivity of CMS to W_R and N_e at high luminosity of 300 fb^{-1} after three years of running should make the discovery region wider. However, to estimate the corresponding discovery region one should devote some efforts to study seriously pile-up effects. The same concerns the analysis of the W_R polarization in case of discovery. This analysis can be done only sufficiently far from the discovery region boundary and with statistics that can be obtained only at high luminosity.

Acknowledgments

We would like to thank S. Slabospitsky for useful discussions.

This work was supported by the Grant RFBR 04-02-16020.

References

- [1] hep-ph/0309200.
- [2] J. C. Pati and A. Salam, Phys. Rev. **D 10**, 275 (1974);
R. N. Mohapatra and J. C. Pati, Phys. Rev. **D 11**, 366 (1975);
G. Senjanovic and R. N. Mohapatra, Phys. Rev. **D 12**, 1502 (1975).
- [3] M. Gell-Mann, P. Ramon and R. Slansky, in *Supergravity*, Ed.by P. van Nieuwenhuizen and D. Freedman (North-Holland 1979);
T. Yanagida, in *Proceedings of the Workshop on the Unified Theory and the Baryon Number in the Universe*, Ed.by O. Sawaga and A. Sugamoto (Tsukuba 1979);
R.N. Mohapatra and G. Senjanovic', Phys. Rev. Lett. **44**, 912, (1980).
- [4] hep-ph/0310238.
- [5] Ho Tso-hsiu, Ching Cheng-rui, and tao Zhi-jian, Phys. Rev. **D 42**, 2265, (1990).

- [6] A. Data, M. Guchait and D. P. Roy, Phys. Rev. **D 47** 961 (1993).
- [7] O. Panella, M. Cannoni, C. Carimalo, and Y. N. Srivastava, Phys. Rev. **D 65**, 035005, (2002).
- [8] B. Mukhopadhyaya, Phys. Rev. **D 49** 1350 (1994); hep-ph/9211240; hep-ph/0104123.
- [9] A. Ferrari *et al.*, Phys. Rev. **D 62**, 031001, (2002).
- [10] J. Polak and M. Zralek, Nucl. Phys. **B363** 385 (1991); A. Pilaftsis, Phys. Rev. **D 52** 459 (1995); M. Czakon, J.Gluza, and M. Zralek, Phys. Lett. **B 458** 355 (1999).
- [11] K. Hagivara *et al.*, Review of Particle Physics, Phys. Rev. **D 66** 1 (2002).
- [12] G. Bell, M. Bander, and A. Soni, Phys. Rev. Lett. **48**, 848 (1982); G. Barenboim, J. Bernabeu, J. Prades and M. Raidal, Phys. Rev. **D 55**, 4213 (1997).
- [13] P. Langacker and S. Uma Sankar, Phys. Rev. **D 40** 1569 (1989).
- [14] S. Abachi *et al.*, D0 Collaboration, Phys. Rev. Lett. **76**, 3271 (1996).
- [15] T. Rizzo, Phys. Rev. **D 50** 325 (1994).
- [16] E. Nardi, E. Roulet, and D. Tommasini, Phys. Lett. **B 344** 225 (1995); J. Gluza *et al.*, Phys. Lett. **B 407** 45 (1997); A. Pilaftsis, Int. J. Mod. Phys. **A 14** 1811 (1999).
- [17] G. Barenboim and M. Raidal, Nucl. Phys. **B 484** 63 (1997) and references therein.
- [18] The Compact Muon Solenoid, Technical Proposal, CERN/LHCC 94-38, 1994.
- [19] The CMS ECAL Technical Design Report, CERN/LHCC 97-33, 1997.
- [20] The CMS HCAL Technical Design Report, CERN/LHCC 97-33, 1997.
- [21] The CMS MUON Technical Design Report, CERN/LHCC 97-33, 1997.
- [22] S. Abdullin, A. Khanov and N. Stepanov, CMSJET 3.2, CMSJET 3.5, CMS TN/94-180.
- [23] T. Sjöstrand, Comput. Phys. Commun. **82** 74 (1994); T. Sjöstrand, Computer Physics Commun. **39** 347 (1986); H.U.Bengtsson and T.Sjöstrand, JETSET, Computer Physics Commun.**43** 367 (1987).
- [24] J. Botts *et al.*, Phys. Lett. **B 304**, 159, (1993).
- [25] S.R. Slabospitsky and L. Sonnenschein, “TopRex generator (version 3.25): Short manual”, Comput.Phys.Comm. **148** 87 (2002); hep-ph/0201292.
- [26] L3 Collaboration, P.Achard *et al.*, Phys. Lett. **B 517** (2001) 67.
- [27] S.I.Bityukov and N.V.Krasnikov, CMS CR 2002/05, hep-ph/0204326; S.I.Bityukov and N.V.Krasnikov, Mod. Phys. Lett **A13** 3235 (1998).